

R econstructing the T riaxial Shapes of D ark M atter H alos from the A nisotropic S patial D istributions of their S ubstructures

Jounghun Lee^{1,2} and X iK ang³

A B S T R A C T

We develop an algorithm for reconstructing the triaxial shapes of dark matter halos from the anisotropic spatial distributions of their substructures. First, we construct an analytic model for the anisotropic spatial distributions of dark halo substructures under the assumption that the tidal field with non-zero trace in the triaxial mass distribution of the host halos generate the substructure bulk motions toward the major principal axes of the hosts. Our analytic model reveals that the degree of anisotropy depends sensitively on the triaxiality of the host halos as well as the correlation between the substructure locations and the tidal shear field. Second, we fit the analytic model to the numerical results from high-resolution N-body simulation with setting the axis ratios of the triaxial host halo as free parameters, and reconstruct the two axis-ratios of the host halos from the best-fit values of the free parameters. The comparison of the reconstructed axis ratios with the numerical results reveals a good agreement. Finally, we conclude that our analytic model may provide a physical understanding of the anisotropic spatial distribution of dark halo substructures and a new way to reconstruct in principle the triaxial shapes of dark matter halos from the observables.

Subject headings: cosmology: theory | large-scale structure of universe

1. I N T R O D U C T I O N

The phenomenon that the satellite galaxies exhibit strong degree of anisotropy in their spatial distributions have recently provoked two-fold controversy: (i) whether the anisotropy

¹School of Physics, Korea Institute for Advanced Study, Seoul 120-43, Korea

²Astronomy Department, School of Earth and Environmental Sciences, Seoul National University, Seoul 151-742, Korea

³Shanghai Astronomical Observatory; the Partner Group of MPA, Nandan Road 80, Shanghai 200030, China

is along the minor or major axes of the host galaxies; (ii) whether it is consistent with the cold dark matter (CDM) paradigm or not.

In fact, the first observational report of this phenomenon dates back to more than three decades ago. Holmberg (1969) analyzed the two dimensional projected positions of the satellite galaxies of nearby spirals, and found an effect (the Holmberg effect) that the satellite locations within the projected radii ~ 50 kpc are quite biased toward the regions around the minor axes of their hosts. In the beginning, the Holmberg effect was suspected not to be real, but due to either the poor number statistics or the projection effects (Hawley & Peebles 1975; Sharp et al. 1979; MacGillivray et al. 1982). It is only very recently when this effect gains supporting evidence for its existence. Sales & Lambas (2004) used a large sample of spiral galaxies and their satellites collected from the Two Degree Field Galaxy Redshift Survey (Colless et al. 2001, 2dFGRS), and found that the satellites have indeed a strong tendency to be located near the minor axes of their hosts as Holmberg claimed more than three decades ago.

In spite of the compelling evidence presented in Sales & Lambas (2004), the Holmberg effect has yet to be confirmed, because another recent report arouse a new suspicion. Brainerd (2004) conducted an analysis of the satellite galaxies about isolated host galaxies in the second data release of the Sloan Digital Sky Survey (Strauss et al. 2002, SDSS), and found that the anisotropy of the satellite spatial distribution is along not the minor but the major axis of the host galaxies, in direct contrast with the Holmberg effect.

A cosmological turmoil surrounding the satellite anisotropy was caused by the other very recent report. Kroupa, Theis, & Boily (2005) claimed that the highly anisotropic spatial distribution of the Milky Way dwarf satellites (Lynden-Bell 1982; Majewski 1994) are not consistent with the CDM picture. Shortly after Kroupa et al. (2005), a flurry of numerical studies on the satellite anisotropy burst out to refute their claim. It was Kang et al. (2005) who for the first time showed by using their high-resolution N-body simulation that the satellites are likely to lie in the plane defined by major and median axes of the halo. Soon Zenter et al. (2005) also demonstrated that the dark halo substructures on galactic scales are preferentially located along the major axes of the triaxial mass distributions of their hosts, proving that the CDM paradigm does not predict the isotropic spatial distribution of satellite galaxies unlike Kroupa et al. (2005) thought (see also, Knebe et al. 2004). Libeskind et al. (2005) also performed a high-resolution simulations of the galactic CDM halos to verify that the satellite anisotropy is not inconsistent with the CDM cosmology.

Despite that the above numerical studies succeeded in saving the CDM model, they did not provide any quantitative explanation for the physical origin of the satellite anisotropy in the CDM context. They all explained that the anisotropy in the satellite distribution may

be caused by the anisotropic infall of materials along the major axes of the host galaxies based on the cosmic web theory (West 1989, Bond, Kofman, & Pogosyan 1996). But, their explanations were inconclusive, making no quantitative prediction for the degree of anisotropy expected on different scales.

Very recently, Lee, Kang, & Jing (2005, hereafter LKJ05) pointed out the incompleteness of the anisotropic infall scenario in their studies of the anisotropic orientations (not the anisotropic locations) of dark halo substructures. They claimed that since the anisotropic infall is a primordial effect, being quickly damped away by the subsequent nonlinear process like the secondary infall, it is unlikely to be the direct cause for the anisotropic orientations of substructures. They assumed that the substructure anisotropic orientations must be caused by the tidal interactions with the gravitational fields in the triaxial mass distribution of their host halos, and constructed an analytic model for the alignments between the major axes of the substructures and their host halos from the physical principles, which turned out to be in good agreement with simulation results.

Motivated by the success of LKJ05 model, here we attempt to construct a similar analytic model for the anisotropic spatial distribution of dark halo substructures assuming that the anisotropy in the spatial locations of substructures are also induced by the tidal interaction with the gravitational field in the triaxial mass distribution of host halos. Our goal is to develop an algorithm for reconstructing the triaxial shapes of host halos from the observable anisotropic spatial distribution of their substructures by using this analytic model.

2. PHYSICAL ANALYSIS

Let us assume that a subhalo lies in the gravitational potential field inside its triaxial host halo. The gravitational field will act on the subhalo position, generating a displacement \mathbf{x} (defined as a vector connecting from the host halo centroid to the subhalo centroid) proportional to \mathbf{r} . Taylor-expanding to second order in the Lagrangian perturbation theory, one can show that $\mathbf{x}_i / q_k T_{ik}$ where $\mathbf{q} = (q_k)$ is the Lagrangian position of the subhalo, and $T = (T_{ik})$ is the tidal shear tensor defined as the second derivative of the gravitational potential: $T_{ik} = \partial_i \partial_k$. This linear perturbation theory implies that the subhalo displacement in the gravitational field is a bulk motion generated by the nonzero quadrupole moment of the triaxial gravitational field.

A question is how the direction of \mathbf{x} is distributed given the tidal shear field T . To answer this, we first consider the covariance $\mathbf{h} \mathbf{x}_i \mathbf{x}_j \mathbf{T}^{-1}$. Using $\mathbf{x}_i / q_k T_{ik}$, we have $\mathbf{h} \mathbf{x}_i \mathbf{x}_j \mathbf{T}^{-1} =$

$h_{ik}q_i T_{ik} T_{lj} i$. If the two tensors, $(q_i q_j)$ and $(T_{ik} T_{kj})$ were mutually independent, then, we would end up with having a simple expression, $h_{ik}q_i T_{ik} T_{lj} i = h_{ik}q_i T_{ik} T_{lj} / T_{ik} T_{kj}$ as $h_{ik}q_i / T_{ik}$. However, it is not necessarily true that $(q_i q_j)$ is uncorrelated with $(T_{ik} T_{kj})$.

To take into consideration the possible correlation between $(q_i q_j)$ and $(T_{ik} T_{kj})$, and to overcome the limited validity of the Lagrangian approximation, we use the following parameterized formula:

$$h_{ik}x_j \mathbb{T} i = \frac{1-s}{3} \mathbb{T}_{ij} + s T_{ik} T_{kj}; \quad (1)$$

where x_i is the rescaled position vector (rescaled in a sense that it does not have a dimension of "length"), $T = (T_{kj})$ is the unit tidal shear tensor with non-zero trace: $T_{ik} = \mathbb{T} j$ and $\text{Tr}(T) \neq 0$ (we use the notation of T to distinguish it from the traceless unit tidal shear tensor \hat{T}), and s is a free parameter in the range of $[-1; 1]$ to quantify the correlation between $(x_i x_j)$ and $(T_{ik} T_{kj})$.

It is worth noting that equation (1) bears a close resemblance to the quadratic formula suggested by Lee & Pen (2001) for the correlation between the dark halo angular momentum $L = (L_i)$ and the unit traceless tidal shear field $\hat{T} = (\hat{T}_{ij})$ defined as $\hat{T}_{ij} = \mathbb{T} j$ with $T_{ij} = T_{ij} - \text{Tr}(T) \mathbb{T}_{ij} = 3$

$$hL_i L_j \mathbb{T} i = \frac{1+c}{3} \mathbb{T}_{ij} - c \hat{T}_{ik} \hat{T}_{kj}; \quad (2)$$

where the correlation parameter c is in the range of $[0; 1]$. LKJ05 used equation (2) to investigate the alignments between the major axes of substructures and their host halos.

Similar as equations (1) and (2) look, it is very important to recognize the key differences between the two. In equation (2), \hat{T} is traceless. Consequently, L is preferentially aligned only with the intermediate principal axis of T . Whereas in equation (2) T has non-zero trace. Consequently, x is preferentially aligned with either the minor or the major principal axis of T : If s is negative, then x is aligned with the minor axis of T . If s is positive, x is aligned with the major axis of T .

Strictly speaking, equation (1) holds only if T and x are smoothed on the same scale. Here, they don't: T is supposed to be smoothed on the host halo mass scale, while x on the substructure radii. For simplicity, here, we just assume that equation (1) still holds, ignoring the difference between the host halo and their substructure smoothing scales.

In a similar manner with LKJ05, assuming that the probability density distribution of $p(x | \mathbb{T})$ is Gaussian, and expressing the position vectors x in terms of the spherical polar coordinates in the principal axis frame of T as $x = (x \sin \theta \cos \phi; x \sin \theta \sin \phi; x \cos \theta)$ where $x = \mathbb{T} j$ and θ, ϕ : the polar and the azimuthal angles of x , respectively, in the principal axis frame of T , we derive the probability density distribution of the cosines of the polar angles,

$p(\cos \theta)$ as:

$$p(\cos \theta) = \frac{1}{2} \frac{Y^3}{2} \sum_{i=1}^2 (1 - s + 3s \frac{2}{i})^{\frac{1}{2}} Z_2^2 \frac{\sin^2 \theta \cos^2 \theta}{1 - s + 3s \frac{2}{1}} + \frac{\sin^2 \theta \sin^2 \theta}{1 - s + 3s \frac{2}{2}} + \frac{\cos^2 \theta}{1 - s + 3s \frac{2}{3}} \stackrel{\frac{3}{2}}{d} : \quad (3)$$

$$\frac{2}{1} + \frac{2}{2} + \frac{2}{3} = 1; \quad \frac{1}{1} + \frac{2}{2} + \frac{3}{3} = \frac{1 + \frac{2}{2} + \frac{3}{3}}{(\frac{2}{1} + \frac{2}{2} + \frac{2}{3})^{1/2}}; \quad (4)$$

where $f_{i=0}^3$ are the three eigenvalues of the tidal shear tensor T in a decreasing order, and $f_{i=1}^3$ are the unit eigenvalues of T defined as $f_{i=1} = (\frac{2}{1} + \frac{2}{2} + \frac{2}{3})^{1/2}$.

In the linear density field, the sum of all the three eigenvalues of the tidal shear tensor equals the linear density contrast: $\frac{1}{1} + \frac{2}{2} + \frac{3}{3} = c$. According to the spherical dynamical collapse model, a gravitational bound object forms when the linear density contrast reaches its critical value, c_c . Hence, one can say that inside the host halo $\frac{1}{1} + \frac{2}{2} + \frac{3}{3} = c_c$. The value of the critical density contrast, c_c , scales with the redshift z as $c_c(z) = D_+(z) c_0$ where D_+ is the growth factor of the density field normalized to be unity at $z = 0$, and c_0 is the critical value at $z = 0$, which depends very weakly on cosmology (Eke, Cole, & Frenk 1996). For example, $c_0 = 1:686$ for the flat universe of closure density. Now, one can rewrite equation (4) as

$$\frac{1}{1} + \frac{2}{2} + \frac{3}{3} = \frac{c}{(\frac{2}{1} + \frac{2}{2} + \frac{2}{3})^{1/2}} \quad (5)$$

As LKJ05 did, we assume further that the tidal shear tensor and the inertia shape tensors of the host halos are strongly correlated in an opposite direction (Lee & Pen 2000; Porciani, Dekel, & Hogg 2002), so that the major and the minor axes of the tidal shear tensor are the major and minor axes of the inertia shape tensor (Lee & Pen 2000; Porciani, Dekel, & Hogg 2002). Under this assumption, equation (3) basically represents the probability density distribution of the cosines of the angles between the position vectors of the substructures and the major principal axes of their host halos. Equations (3) reveals that $p(\cos \theta)$ depends sensitively on the value of s : If $\frac{1}{1} - s < 0$, x is aligned with the major axis of the host halo (the minor axis of T); If $0 < s < 1$, x is aligned with the minor axis of the host halo (the major axis of T); If $s = 0$, there is no alignment between x and any principal axis of the host halo.

Note that even when $s \neq 0$, it is possible to have no alignment between x and the host halo axes. The distribution $p(\cos \theta)$ depends not only on the value of s but also on the unit eigenvalues with non-zero trace, $f_{i=0}^3$. For the case of the traceless eigenvalues of $f_{i=0}^3$

which satisfies the two constraints: $\sum_{i=0}^3 \hat{\gamma}_i = 0$ and $\sum_{i=0}^3 \hat{\gamma}_i p_i = 1$ (see x2 in LK J05), their values are well approximated as the average $\hat{\gamma}_1 = \hat{\gamma}_3 = 1/2$ and $\hat{\gamma}_2 = 0$ regardless of the original values of f_{sg}^3 . However, for f_{sg}^3 , the constraints (eq.[4]) are expressed in terms of the original values of f_{sg}^3 . Therefore, even when the correlation parameter ϵ has the maximum absolute value (i.e., $\epsilon_{\text{sj}} = 1$), if the host halo has almost spherical shapes satisfying $\gamma_1 = \gamma_2 = \gamma_3 = 0$, then $p(\cos \theta)$ becomes uniform, implying no anisotropy in the spatial distribution of substructures.

3. HALO SHAPE RECONSTRUCTION

To find $p(\cos \theta)$ numerically, we use the same numerical data as used in LK J05 which were generated by P^3M N-body simulations with 256^3 particles in a $100h^{-1}\text{Mpc}$ cube (Jing & Suto 1998, 2000) for the ‘concordance’ CDM cosmology with $\Omega_0 = 0.3$, $\sigma_8 = 0.7$, and $h = 0.7$. In the simulation data, we selected four dark halos on mass scales around $5 \times 10^{14}h^{-1}\text{M}_\odot$, and identified the self-bound substructures in each host halo by using the SUBFIND routine of Springel et al. (2001). For the detailed descriptions of the N-body simulations and the subhalo identification procedure, see x3 in LK J05.

For each host halo selected in the numerical data, we compute the inertia shape tensor $I_{ij} = \sum_m r_{i,m} r_{j,m}$ and determine the major principal axis by finding the eigenvector \hat{e}_h of (I_{ij}) corresponding to the largest eigenvalue. In each host halo principal axis frame, we measure the unit position vectors of the subhalos \hat{x}_s , and the cosines of the angles, θ_{hsj} , between the major axis of the host halo and the locations of their subhalos by computing $\cos \theta_{hsj} = \hat{e}_h \cdot \hat{x}_s$. We find the probability density distribution, $p(\cos \theta)$ by counting the subhalo number density as a function of $\cos \theta$.

We fit our analytic model (eq.[1]) to this numerically determined $p(\cos \theta)$ with setting the three parameters, γ_1, γ_2 (γ_3 is not independent according to eq.[4]) and ϵ as free, and determine the best-fit values of the free parameters by means of the χ^2 statistics. We perform this procedure for each individual host halo (CL# 1, CL# 2, CL# 3, CL# 4) separately at four different redshifts ($z = 0.05; 1.15$).

Figure 1 plots the final fitting result. In each panel, the histogram represents the numerically measured $p(\cos \theta)$, while the (red) solid curve corresponds to the analytic distribution (eq.[3]) with the best-fit correlation parameters. As one can see, for all cases, the best-fit correlation parameter has a negative value. In other words, the dark halo substructures are preferentially located near the major axis of their host halos, consistent with previous numerical findings (Knebe et al. 2004; Zenter et al. 2005; Libeskind et al. 2005). Indeed, the

analytic distributions agree with the numerical results for all four clusters at all redshifts quite well.

As a final step, we reconstruct the triaxial shapes of the four host halos from their distributions $p(\cos \phi)$. For this purpose, we adopt the following formula suggested recently by Lee, Jing & Suto (2005):

$$\frac{a_2}{a_1} = \frac{1 - D_{+2}}{1 - D_{+3}}^{1/2}; \quad \frac{a_3}{a_1} = \frac{1 - D_{+1}}{1 - D_{+3}}^{1/2} \quad (6)$$

where a_1, a_2, a_3 represent the three axis lengths of the triaxial host halos in a decreasing order. Equation (6) basically links the two axes ratios of the triaxial host halos to the eigenvalues of the tidal shear tensors. According to this equation, once $f_{\text{ig}_{i=3}^3}$ is determined, then one can reconstruct the axis ratios of the host halos.

Equations (4) and (5) allow one to determine the values of $f_{\text{ig}_{i=3}^3}$ from the best-fit values of $f_{\text{ig}_{i=3}^3}$ as

$$1 = \frac{c_1}{1 + c_2 + c_3}; \quad 2 = \frac{c_2}{1 + c_2 + c_3}; \quad 3 = \frac{c_3}{1 + c_2 + c_3} \quad (7)$$

We use $c = 1.686$ as an approximation and the best-fit values of c_1, c_2, c_3 to determine the values of a_1, a_2, a_3 using equation (7) for each host halo, and finally reconstruct the axis ratios of the host halo using equation (6). With the above method, we finally reconstruct the two axis ratios of all four clusters at four redshifts.

Figure 2 plots the intermediate major axis ratio vs. the minor-to-major axis ratios of the four clusters at four redshifts. In each panel, the (red) triangle dot represents the reconstructed axis ratios by the above algorithm, and the (blue) square dot is the original axis ratios from simulations. Although the reconstruction does not look perfect, it works quite satisfactorily, especially given the all the approximations used in the algorithm. It is obvious that at least one of the two axis ratios fairly accurately reconstructed. We note that for the case of $s' = 1$, the difference between $a_2=a_1$ and $a_2=a_1$ is relatively large, which trend is also reconstructed well by our algorithm.

4. DISCUSSIONS AND CONCLUSIONS

Our achievements are summarized as follows: (i) we construct an analytic model for the anisotropic spatial distribution of dark halo substructures; (ii) we confirm numerically that the dark halo substructures have a strong propensity to be located near the major axes

of their host halos; (iii) we develop an algorithm to reconstruct the triaxial shapes of dark halos from the anisotropic spatial distribution of their substructures.

Successful as are our analytic model and the reconstruction algorithm based on it, it is worth noting a couple of its inconsistencies. First, as mentioned in x2, equation (3) holds only when the tidal shear field is smoothed on the substructure radii. We ignored the smoothing scale difference, which should cause some scatters in the measurement of the correlation parameters. Second, we adopted the spherical collapse condition $\alpha_1 + \alpha_2 + \alpha_3 = \alpha_c = 1.686$ even though we consider triaxial dark matter halos. Definitely, it will be necessary to refine our analytic model further, accounting for these two inconsistencies.

Now that we proved that it can reconstruct in principle the axis-ratios of triaxial dark halos from the anisotropic spatial distribution of substructures, it is worth discussing about how to apply the algorithm to real data from observations of such as the weak gravitational lensing. In our analytic model, the substructure positions are defined in the real three dimensional space relative to the principal axes of host halos, which is, however, very difficult to determine in practice. In observations they are measured in the two dimensional space projected along the line-of-sight direction which is not necessarily coincident with the host halo principal axis. Therefore, to apply our reconstruction algorithm to real data, it will be necessary first to find an analytic expression of the substructure spatial distributions in the general non-principal axis frame and to account for the effect of projection along the line-of-sight. Our future work is in this direction, and we wish to report it elsewhere soon.

Another direction is our future work toward is to explain the Holmberg effect. As shown, our analytic model for the substructure spatial distribution (eq. [3]) is characterized by the single correlation parameter, s . By investigating what physical mechanism caused the correlation parameter to change their signs, it might be possible to explain the Holmberg effect theoretically.

Finally, we conclude that our analytic model may provide a physical quantitative understanding of the anisotropic spatial distribution of dark halo substructures, and will allow us to determine in principle the axis-ratios of triaxial dark halos from the observables.

We thank Y. Jing for generously providing simulation data and many useful discussions. J.L. is supported by the research grant No. R01-2005-000-10610-0 from the Basic Research Program of the Korea Science and Engineering Foundation. X.K. is partly supported by NKBRSF (G 19990754), by NSFC (Nos. 10125314, 10373012), and by Shanghai Key Projects in Basic Research (No. 04JC14079).

R E F E R E N C E S

Bond, J.R. 1987, in *Nearly Normal Galaxies*, ed. S. Faber (New York: Springer), 388

Bond, J., Kofman, L., & Pogosyan, D. 1996, *Nature*, 380, 603

Brainerd, T.G. 2004, preprint (astro-ph/0408559)

Colless, M., Dalton, G., Maddox, S., Sutherland, W., & the 2dF collaboration. 2001, *MNRAS*, 328, 1039

Eke, V., Cole, S., & Frenk, C. 1996, *MNRAS*, 283, 263

Fuller, T.M., West, M.J., & Bridges, T.J. 1999, *ApJ*, 519, 22,

Hawley, D.L., & Peebles, P.J.E. 1975, *AJ*, 80, 477

Holmberg, E. 1969, *Ark. Astron.*, 5, 305

Jing, Y.P. & Suto, Y. 1998, *ApJ*, 503, L9

Jing, Y.P. & Suto, Y. 2000, *ApJ*, 529, L69

Jing, Y.P. & Suto, Y. 2002, *ApJ*, 574, 538

Kroupa, P., Theis, C., & Boily, C.M. 2005, *A&A*, 431, 517

Knebe, A. et al. 2004, *ApJ*, 603, 7

Lee, J., Kang, X., & Jing, Y.P. 2005, preprint (astro-ph/0503136)

Lee, J., Jing, Y.P. & Suto, Y. 2005, preprint (astro-ph/0504623)

Lee, J. & Pen, U.L. 2000, *ApJ*, 532, L5

Lee, J. & Pen, U.L. 2001, *ApJ*, 555, 106

Lynden-Bell, D. 1982, *Obs.*, 102, 202

Libeskind, N.I., Frenk, C.S., Cole, S., Helly, J.C., Jenkins, A., Navarro, J.F., & Power, C. 2005, preprint (astro-ph/0503400)

MacGillivray, H.T., Dodd, R.J., McNally, B.V., & Cowin, H.G. 1982, *MNRAS*, 198, 605

Majewski, S.R. 1994, *ApJ*, 431, L17

Mo, H.J., Mao, S., & White, S.D.M. 1998, *MNRAS*, 297, L71

Porciani, C., Dekel, A., & Homan, Y. 2002, MNRAS, 332, 325

Sharp, N. A., Lin, D. N. C., & White, S. D. M. 1979, MNRAS, 187, 287

Sales, L. & Lambas, D. G. 2004, MNRAS, 348, 1236

Strass, M. A., Weinberg, D. H., Lupton, R. H., & the SDSS collaboration, 2002, AJ, 124, 1810

Springel, V., White, S. D. M., Tormen, G., Kauffmann, G. 2001, MNRAS, 328, 726

Valtonen, M., Taurikorpi, P., & Argue, A. 1978, AJ, 83, 135

West, M. J. 1989, ApJ, 347, 610

West, M. J. 1994, MNRAS, 268, 79

Zaritsky, D., Smith, R., Frenk, C. & White, S. D. M. 1997, ApJ, 478, L53

Zenter, A. R., Kravtsov, A. V., Gnedin, O. Y., & Klypin, A. A. 2005, preprint (astro-ph/0502496)

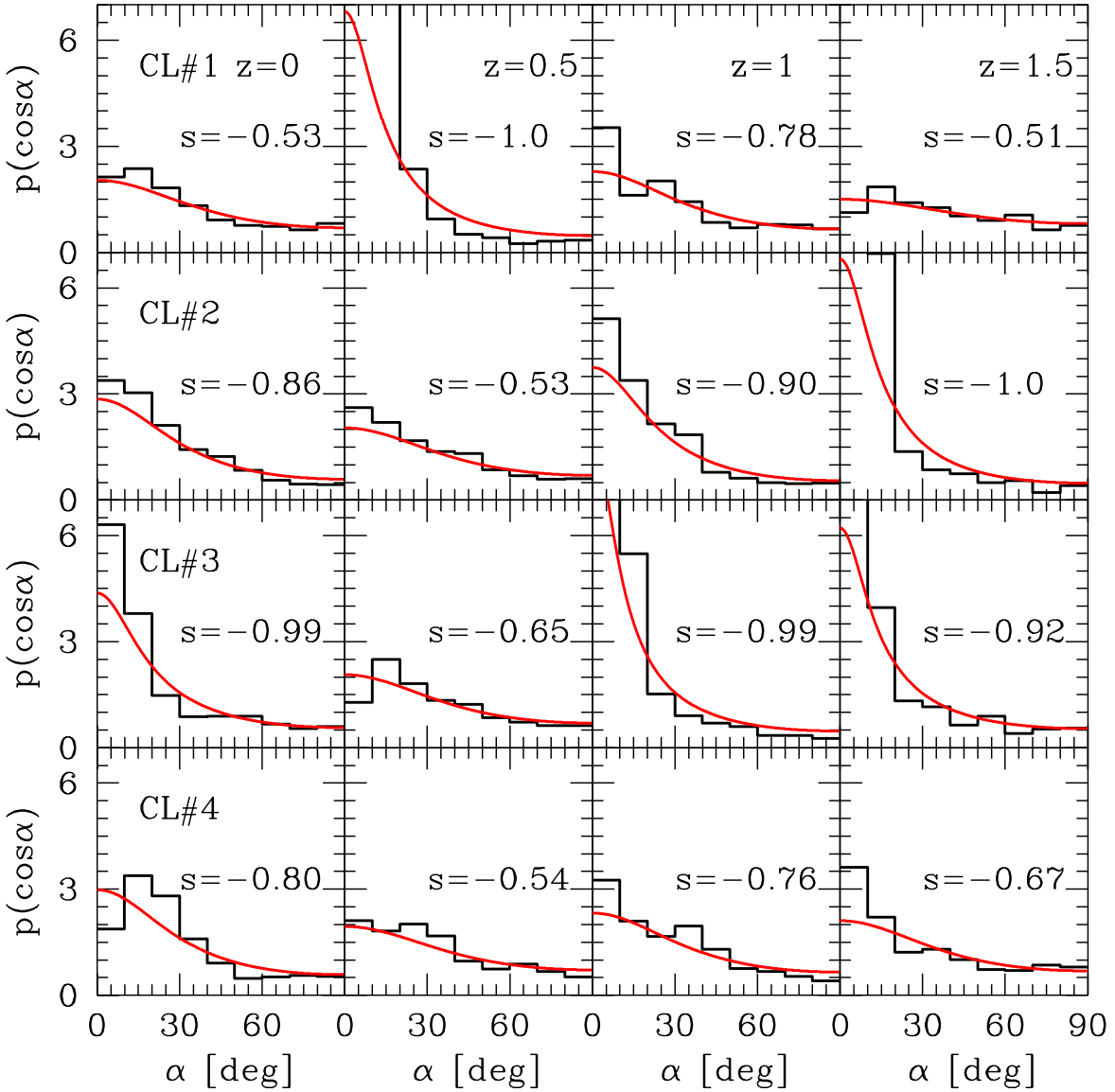


Fig. 1. Probability density distributions of the angles between the major axes of four individual host halos and the position vectors of their substructures at four different epochs; $z = 0; 0.5; 1$ and 1.5 . In each panel, the histogram represents the simulation results, and the (red) solid line represent the theoretical prediction (3).

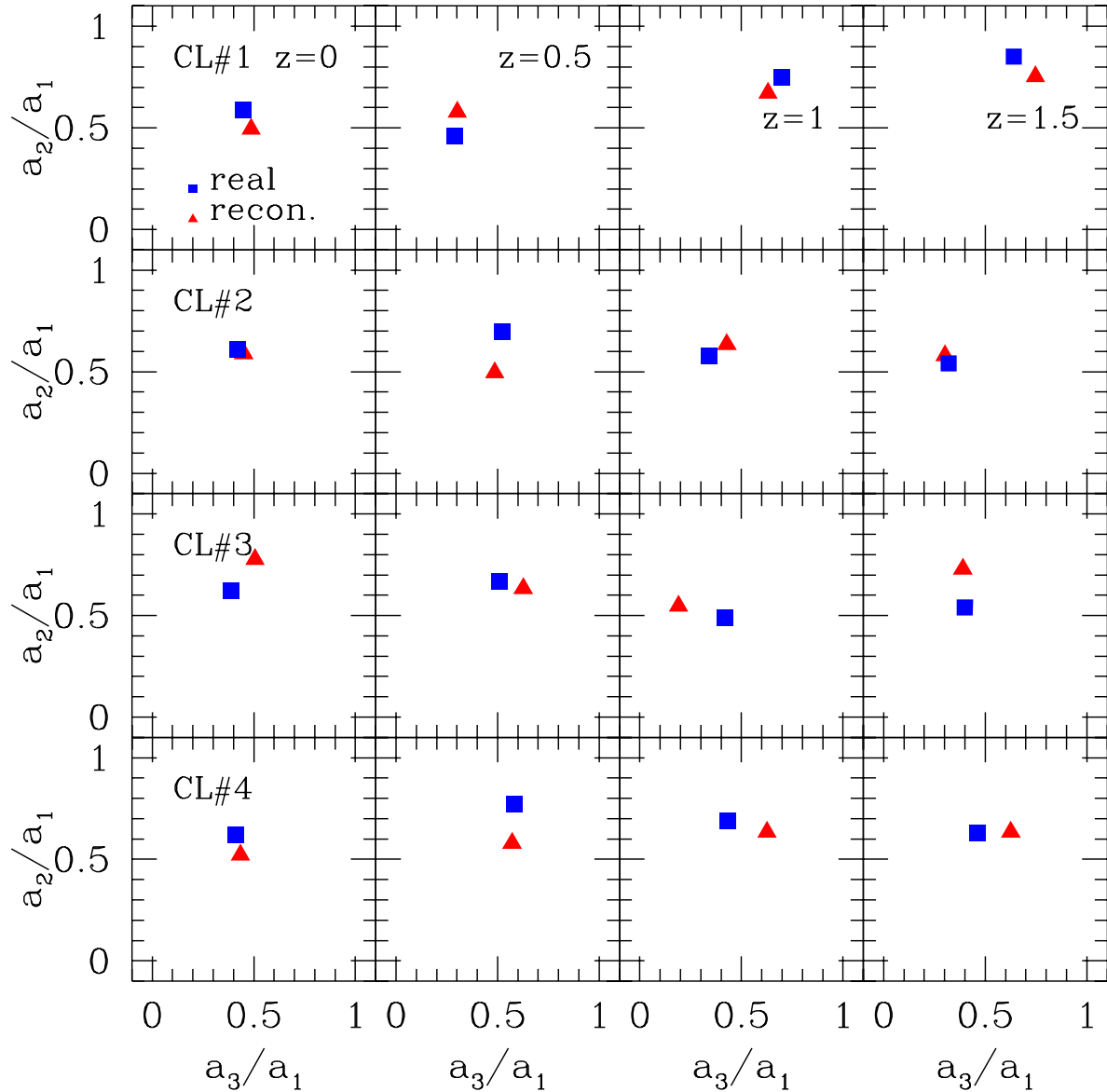


Fig. 2.1 A xis-ratios of four individual clusters at four di erent epochs; In each panel, the square represents the real axis ratio measured in simulations while the triangle represents the reconstructed axis ratio.